Quantum Oscillations in the Layer Structure of Thin Metal Films

P. Czoschke,[1,2] Hawoong Hong,[2] L. Basile,[1,2] and T.-C. Chiang[1,2]

[1]*Department of Physics, University of Illinois at Urbana-Champaign, 1110 W. Green Street, Urbana, Illinois 61801-3080, USA*
[2]*Frederick Seitz Materials Research Laboratory, University of Illinois at Urbana-Champaign, 104 S. Goodwin Avenue, Urbana, Illinois 61801-2902, USA*

(Received 7 July 2003; published 25 November 2003)

Understanding the underlying physical principles that determine the internal structure of objects at the atomic scale is critical for the advancement of nanoscale science. We have performed synchrotron x-ray diffraction studies to determine the structural properties of smooth Pb films with varying thicknesses of 6 to 18 monolayers deposited on a Si(111) substrate at 110 K. We observe quasibilayer variations in the atomic interlayer spacings of the films consistent with charge density oscillations due to quantum confinement of conduction electrons and surface-interface interference effects. Quantum oscillations in atomic step height are also deduced.

DOI: 10.1103/PhysRevLett.91.226801 PACS numbers: 73.21.Fg, 61.10.Kw, 68.55.Jk

As the physical size of a structure approaches the atomic scale, nonclassical effects become increasingly important and departure from the bulk properties can be expected. In particular, quantum electronic effects have been shown to play an important role in determining the growth behavior and morphology of metal films [1–4]. Given the importance of electronic effects in these systems, it has been predicted that quantum size effects will manifest themselves in the layer structure of the film as well, causing variations in the atomic interlayer spacings [5]. However, evidence for such effects has been limited to the measurement of step heights by scanning tunneling microscopy (STM) and helium atom scattering (HAS) [6–8], both of which only probe the top surface of the film and provide little information on internal film structure. Here we present a study of smooth Pb films deposited on a Si(111) substrate using x rays from a synchrotron source. Since x rays fully penetrate the film, information on the internal atomic layer structure as well as the buried film-substrate interface is probed. The results show lattice distortions with a quasibilayer periodicity which can be explained with a physical model based on confinement of the film's conduction electrons to a quantum well and interference effects between the film boundaries. The absolute film thicknesses are also determined, which indicate the presence of substantial oscillatory step height variations on the film surface.

We determined the interlayer spacings in the metal films by measuring, *in situ*, the integrated specular reflectivity rod using 19.9 keV x rays from an undulator source at Sector 33, UNICAT (University-National Laboratory-Industry Collaborative Access Team), Advanced Photon Source, Argonne National Laboratory. The substrate was prepared by depositing 4.5 Å Pb onto a clean Si(111)-(7×7) reconstructed surface at room temperature, followed by a 10 min anneal at 415 °C. This process results in the $\frac{1}{3}$-ML (monolayer) coverage, commensurate Pb/Si(111)-$(\sqrt{3} \times \sqrt{3})R30°$ surface [9,10], which was verified by examining both reflection high energy electron diffraction patterns, in-plane x-ray superstructure peaks, and the x-ray reflectivity rod. Pb films were deposited incrementally using an effusion cell at a rate of 0.652 Å/min, which was calibrated using a quartz crystal thickness monitor. The sample temperature was maintained at 110 K for the duration of the experiments, measured via a thermocouple attached to the clips holding the sample. The specular rod profile was measured using either the ω-scan method or a series of parallel line scans to obtain the background-subtracted integrated intensity [11,12]. Different momentum transfers were selected by varying the incident beam angle and exiting scattering angle (which are equal for the specular condition) with a six-circle goniometer. The reflectivity profiles for nominal coverages $N = 6$–18 Pb ML are shown in Fig. 1. The steep tails at perpendicular momentum transfer $l = 3$ and 9 are the edges of the Si(111) and (333) Bragg peaks, respectively, between which are multilayer interference fringes due to the Pb overlayers. Monolayer resolution is evident as some of the interference minima turn into near maxima with a monolayer increment in film thickness. These results imply that the films follow a smooth layer-by-layer growth mode, which is in stark contrast to the "magic thickness" effect seen for growth at higher temperatures [13].

The most unusual features of the profiles in Fig. 1 are the relatively pronounced fringes at $l \approx 4.8$ and 8.1, marked by inverted triangles, which are located approximately halfway between the bulk Pb(111), (222), and (333) Bragg positions at $l \approx 3.3$, 6.6, and 9.9, respectively. The proximity of the features to the half-order point for Pb is an indication of a quasibilayer superperiodicity to the lattice in the z direction (the surface normal). This effect is analogous to the superstructure peaks found at in-plane fractional order positions due to surface reconstructions [11]. However, in our case the superperiod, or periodic lattice distortion, is in the direction of the

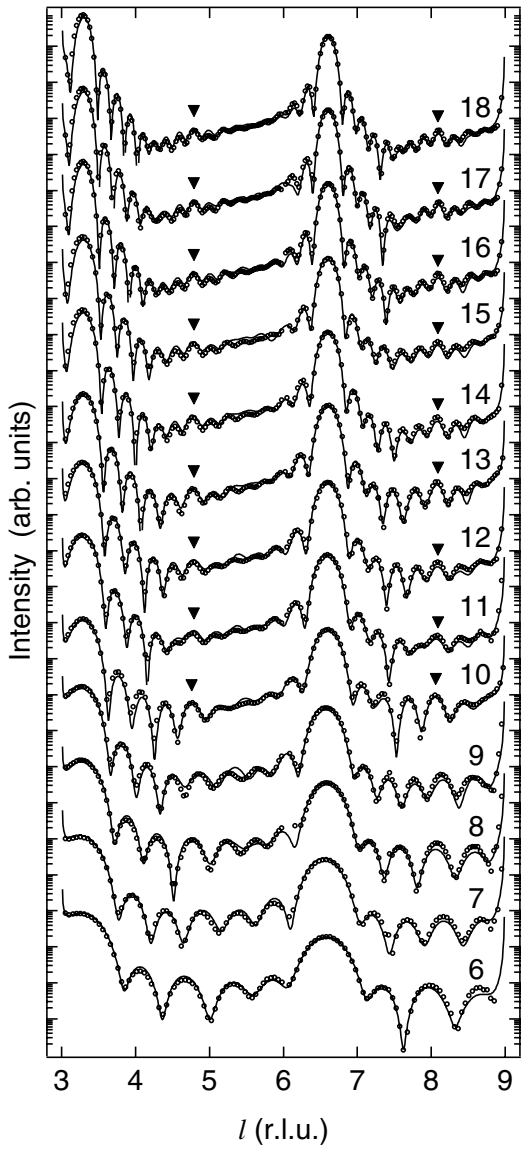

FIG. 1. X-ray reflectivity data (circles) for Pb films with thicknesses 6–18 ML and fits using the model described in the text (solid curves). Nominal coverages are indicated for each curve. The abscissa is the momentum transfer along the surface normal in Si reciprocal lattice units (1 r.l.u. = 0.668 Å^{-1}). The tails of the sharp Si(111) and (333) Bragg peaks can be seen at $l = 3$ and $l = 9$, and the large peaks at $l \approx 3.3$, 6.6, and 9.9 (not shown) correspond to the Pb(111), (222), and (333) Bragg positions, respectively, halfway between which the prominent half-order features can be seen (inverted triangles). As discussed in the text, such features are indicative of a quasibilayer superperiod in the direction normal to the surface.

surface normal. The intensity of the superstructure peak is much lower than the Pb Bragg peaks, indicating that the quasibilayer distortion is relatively weak and possibly damped. Damping is also implied because bulk Pb does not exhibit such distortions.

The quasibilayer lattice distortion can be explained in terms of electronic charge density variations in the film by recognizing that confinement of the conduction electrons in the metal film by its boundaries leads to a one-dimensional quantum well. As a result, the charge density in the film differs from the perfectly periodic bulk charge density. A charge imbalance or asymmetry about an atomic plane exerts an electronic force that can move the atomic plane away from the ideal bulk position. Within a linear response regime appropriate for small lattice distortions, the movement of an atomic plane is proportional to the derivative of the local charge density. To formulate this idea, we approximate the system by a free-electron gas confined by two infinite potential barriers at $z = 0$ and D. The allowed states then become quantized, where wave vectors in the z direction can take on only the discrete values

$$k_z = \frac{\pi n}{D}, \qquad n = 1, 2, 3, \ldots, \tag{1}$$

leading to the formation of Fermi disks or subbands at each k_z value. The charge density at a point z in the quantum well can be found by summing over the states of all occupied subbands

$$\rho(z) \propto \sum_{n=1}^{n_0} (k_F^2 - k_z^2)\sin^2(k_z z), \tag{2}$$

where k_F is the Fermi wave vector and $n_0 = \text{int}(k_F D/\pi)$ is the quantum number for the highest occupied subband. The normalized (fractional) spatial variations in the charge density are then

$$\delta\rho(z) \equiv \frac{\rho(z) - \langle\rho(z)\rangle}{\langle\rho(z)\rangle} \tag{3}$$

$$= -\frac{1}{\sum_{n=1}^{n_0}(k_F^2 - k_z^2)}\left(k_F^2 + \frac{1}{4}\frac{\partial^2}{\partial z^2}\right)S_D\left(\frac{2\pi z}{D}\right), \tag{4}$$

where $\langle\cdots\rangle$ indicates the average over z. S_D is the dimensionless geometric sum

$$S_D(x) \equiv \sum_{n=1}^{n_0} \cos(nx) \tag{5}$$

$$= \frac{1}{2}\sin(n_0 x)\cot\left(\frac{x}{2}\right) - \sin^2\left(\frac{n_0 x}{2}\right), \tag{6}$$

which gives rise to a n_0-slit interference pattern with a characteristic wavelength of $D/n_0 \approx \pi/k_F = \lambda_F/2$ (one-half of the Fermi wavelength). An example of this effect for one of the films studied here, with $N = 10$, can be seen in Fig. 2(a). The oscillations are similar to the usual Friedel oscillations. They are damped away from the boundaries, but there is considerable interaction (or interference) between the two boundaries for the thickness ranges investigated here.

In reality the potential barriers defining the quantum well are not infinite in magnitude, allowing charge to tunnel or "spill out" past the well boundaries. This effect can be approximated by letting the well expand slightly at

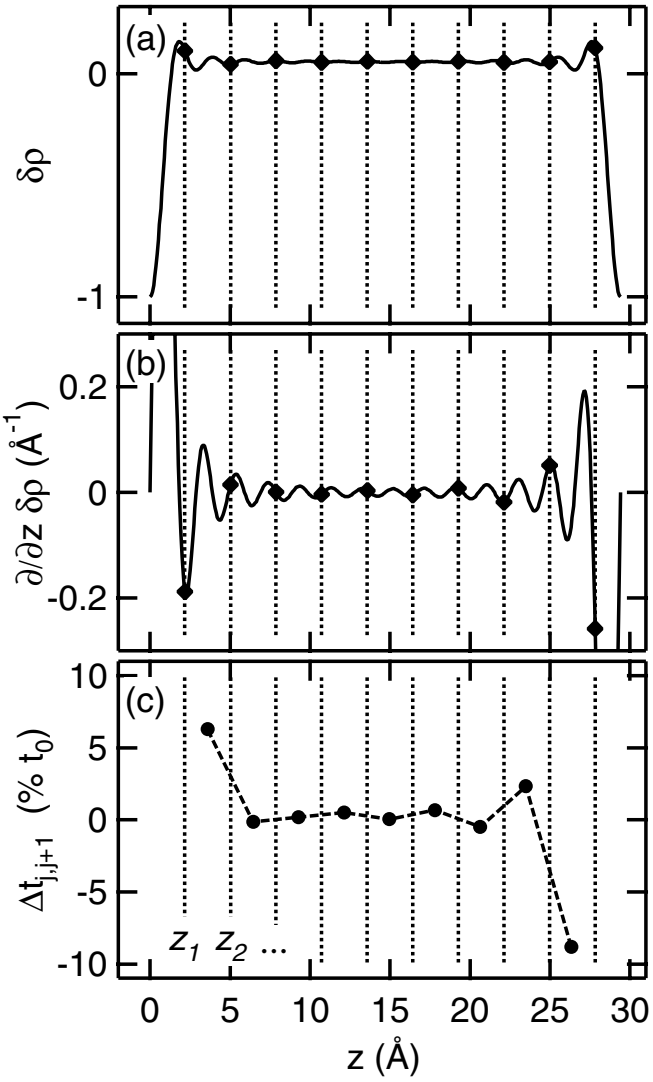

FIG. 2. Because of the confinement of conduction electrons in a quantum well ($N = 10$), oscillations in the electron density (a) will be present in the film. The displacement of each atomic plane is proportional to the first derivative (b) of these density variations, from which the changes in individual interlayer spacings (c) can be calculated. The abscissa is the distance into the quantum well, where $z = 0$ is the film-substrate well boundary. The ideal positions of the atomic layers, z_j, are marked with vertical dotted lines and in (a) and (b) the intersection of these positions with the curves are marked with diamonds. All curves and values are calculated using the model parameters resulting from the fit to the experimental data for $N = 10$ shown in Fig. 1.

both interfaces. Define the quantum well width to be

$$D = \Delta_s + Nt + \Delta_0, \tag{7}$$

where t is the average atomic layer thickness in the film, and Δ_s and Δ_0 are parameters that account for charge "spillage" past the substrate-film and vacuum-film interfaces, respectively. The usage of charge spillage parameters is similar to the boundary phase shifts that are often employed, instead, in discussions of quantum wells [14]. In the absence of any variations in the interlayer spacings, the atomic planes would be found at the positions

$$z_j = \Delta_s + (j - \tfrac{1}{2})t, \qquad j = 1, 2, \ldots, N, \tag{8}$$

with $j = 1$ being the atomic layer next to the substrate.

The lattice distortion is proportional to the derivative of the charge density variations. Of primary interest here is the change in atomic layer spacing between layers j and $j + 1$ from the average spacing t, which is given by

$$\Delta t_{j,j+1} = A\left[\frac{\partial}{\partial z}\delta\rho(z_{j+1}) - \frac{\partial}{\partial z}\delta\rho(z_j)\right], \tag{9}$$

where a response coefficient, A, has been included. The model therefore has only four parameters for the film: A, Δ_s, Δ_0, and t. We allow the possibility that the average layer spacing t can differ from the bulk value. This is physically reasonable and, furthermore, necessary as the positions of the measured Pb Bragg peaks in Fig. 1 differ slightly from the predicted positions based on the bulk Pb lattice constant. The experimental data in Fig. 1 were fit using a standard kinematic model [15–17] with the lattice distortion given by Eq. (9). Film roughness is allowed in the model as a distribution of thicknesses, but is fairly small from the fits. The four model parameters for each thickness N from the fits yield consistent values across the range of thicknesses with $A = 76 \pm 8$ Å^2, $\Delta_s = 0.75 \pm 0.03$ Å, and $\Delta_0 = 0.18 \pm 0.05$ Å, where errors correspond to the standard deviation of the spread of fitted results. The fitted value for $t = 2.849 \pm 0.004$ Å is just slightly different from the bulk value $t_0 = 2.84$ Å. The calculated reflectivity profiles based on the model are shown in Fig. 1 as solid curves. They describe the data very well over the wide thickness range and, most importantly, they reproduce the half-order features discussed above.

The model thus reproduces the quasibilayer periodicity in the film structure. A physical explanation follows. In addition to $\delta\rho(z)$, Fig. 2 shows, for $N = 10$, the first derivative of $\delta\rho(z)$, which is proportional to the distortive force, and the calculated change in atomic layer spacing, $\Delta t_{j,j+1}$. All of these quantities exhibit damped oscillations at a wavelength of $\lambda_F/2 = 1.98$ Å, which is close to $\frac{2}{3}$ the expected bulk interlayer spacing of $t_0 = 2.84$ Å. Every two layers of Pb will thus roughly correspond to an integral number of oscillations in the charge density, resulting in an approximate bilayer periodicity of the lattice distortion given by Eq. (9). The quasibilayer periodicity in the film structure is most obvious in the layer relaxations near the surface, where the layers alternate between expansion and contraction (Fig. 2(c)). In addition, the interlayer spacing between the two Pb layers of the film closest to the silicon substrate ($\Delta t_{1,2}$) shows a substantial expansion, which is not easily accessible by other experimental techniques. Layer relaxation profiles for other thicknesses are qualitatively similar.

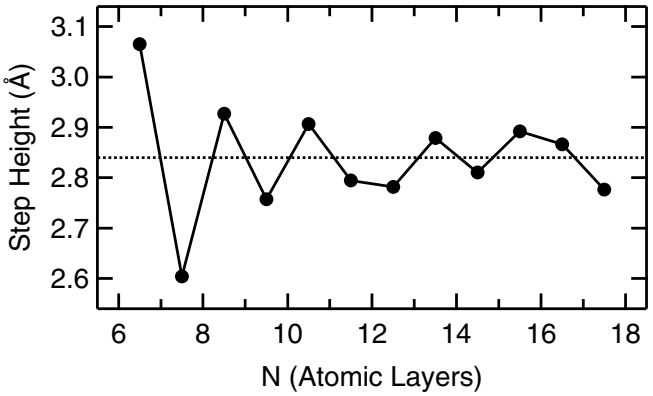

FIG. 3. Step heights that would be observed in an STM or HAS experiment. The points are derived from the difference between the net thicknesses of films differing by one atomic layer and are positioned between the two relevant film thicknesses. The horizontal dotted line is positioned at the bulk Pb(111) interlayer spacing, $t_0 = 2.84$ Å. Quasibilayer oscillations are evident, consistent with the results seen in STM and HAS studies.

These results are also found to be consistent with previous STM and HAS experiments, which sense only the top surface morphology. Using such techniques, the step heights at the sample surface are recorded by scanning over or scattering from regions of the same electron density on the surface. To extract from our results what such an experiment might detect, apparent step heights were deduced by taking the difference between two net film thicknesses, defined as the sum of all the adjusted layer thicknesses plus the charge spillage into the vacuum, Δ_0. The results are shown in Fig. 3. The quasibilayer oscillations in step height as a function of thickness are again readily apparent and are similar to what has been observed [6–8], although exact correspondence is not expected. Such oscillations are thus a consequence of the more complicated structural modifications due to the oscillations in the charge density present throughout the film that arise from quantum interference between the two film interfaces.

The x-ray diffraction results presented in this study show that the internal structure of thin metal films can be significantly modified as a result of quantum confinement and interference effects. Although smooth two-dimensional films were studied in this experiment, it is reasonable to expect a similar phenomenon for three-dimensional nano-objects as well. An important finding from this experiment, however, is that the structural modifications due to such quantum size effects can penetrate many layers into the object and occur at all of its boundaries. Such effects must therefore be accounted for and considered in the design and applications of metallic nanoscale objects.

This work is supported by the U.S. Department of Energy (Grant No. DEFG02-91ER45439). The UNICAT facility at the Advanced Photon Source (APS) is supported by the University of Illinois at Urbana-Champaign, Frederick Seitz Materials Research Laboratory (U.S. DOE, and the State of Illinois-IBHE-HECA), the Oak Ridge National Laboratory (U.S. DOE under contract with UT-Battelle LLC), the National Institute of Standards and Technology (U.S. Department of Commerce), and UOP LLC. The APS is supported by the U.S. DOE under Contract No. W-31-109-ENG-38. We also acknowledge partial equipment and personnel support from the Petroleum Research Fund, administered by the American Chemical Society, and the U.S. National Science Foundation (Grant No. DMR-02-03003).

[1] D.-A. Luh, T. Miller, J. J. Paggel, M. Y. Chou, and T.-C. Chiang, Science **292**, 1131 (2001).
[2] K. Budde, E. Abram, V. Yeh, and M. C. Tringides, Phys. Rev. B **61**, R10 602 (2000).
[3] A. Mans, J. H. Dil, A. R. H. F. Ettema, and H. H. Weitering, Phys. Rev. B **66**, 195410 (2002).
[4] H. Hong, C.-M. Wei, M. Y. Chou, Z. Wu, L. Basile, H. Chen, M. Holt, and T.-C. Chiang, Phys. Rev. Lett. **90**, 076104 (2003).
[5] P. J. Feibelman, Phys. Rev. B **27**, 1991 (1983).
[6] W. B. Su, S. H. Chang, W. B. Jian, C. S. Chang, L. J. Chen, and T. T. Tsong, Phys. Rev. Lett. **86**, 5116 (2001).
[7] A. Crottini, D. Cvetko, L. Floreano, R. Gotter, A. Morgante, and F. Tommasini, Phys. Rev. Lett. **79**, 1527 (1997).
[8] J. Braun and J. P. Toennies, Surf. Sci. **384**, L858 (1997).
[9] J. A. Carlisle, T. Miller, and T.-C. Chiang, Phys. Rev. B **45**, 3400 (1992).
[10] F. Grey, R. Feidenhans'l, M. Nielsen, and R. L. Johnson, Colloque de Physique **C7**, 181 (1989).
[11] I. K. Robinson and D. J. Tweet, Rep. Prog. Phys. **55**, 599 (1992).
[12] R. Feidenhans'l, Surf. Sci. Rep. **10**, 105 (1989).
[13] M. Hupalo, V. Yeh, L. Berbil-Bautista, S. Kremmer, E. Abram, and M. C. Tringides, Phys. Rev. B **64**, 155307 (2001).
[14] J. J. Paggel, T. Miller, and T.-C. Chiang, Science **283**, 1709 (1999).
[15] B. E. Warren, *X-ray Diffraction* (Dover, New York, 1969).
[16] I. K. Robinson and E. Vlieg, Surf. Sci. **261**, 123 (1992).
[17] E. D. Specht and F. J. Walker, J. Appl. Crystallogr. **26**, 166 (1993).